

# Thermal Analysis of Toroidal Transformers Using Finite Element Method

Adrian T. Pleşca

**Abstract**—In this paper a three dimensional thermal model of a power toroidal transformer is proposed for both steady-state or transient conditions. The influence of electric current and ambient temperature on the temperature distribution, has been investigated. To validate the three dimensional thermal model, some experimental tests have been done. There is a good correlation between experimental and simulation results.

**Keywords**—Temperature distribution, thermal analysis, toroidal transformer.

## I. INTRODUCTION

THE transformers have different configurations but the core shapes have two main types: EI laminations and toroidal cores. In selecting one, the criteria are: the application, cost, efficiency, size, shape and volume. Toroidal construction has advantages related to size, volume, the winding occupies the full periphery of the core, resulting in reduced leakage inductance and stray magnetic fields and a lower air gap. The first transformer built by Faraday in 1831 had a toroidal core and even the first industrial grade transformer was also wound in toroidal core (Ganz factory, in 1885). At present, toroidal transformers are to be found in modern applications, especially in the low-voltage or low power for electronics equipments, audio systems and avionics. Although the toroidal transformers have many advantages over the classical ones, there are disadvantages to overcome in order to extend their use at medium and high power, as the cost, the difficulty of the winding and the limited published experience [1]. To study the thermal aspects of the transformers there are several thermal model, as: hot spot temperature model, IEEE alternative thermal model, the top oil model, the ANSI top-oil-rise model, the semi-physical model, the Pierce's model, the thermal-electrical model. Some of the thermal models are compared with each other in [2]. Classical transformers are largely studied from the point of view of thermal aspects, as in [2]-[4]. A survey of researches reveals the future trends and the continued interest in application of advanced techniques for transformer design optimization. Artificial Intelligence techniques have been extensively used in order to cope with the complex problem of transformer design optimization, including toroidal core transformers [5]. The toroidal transformers are less studied but there are comparisons between the thermal aspects for toroidal

and conventional types transformers in various configurations, considering experimental analysis of the effect of temperature on parameters of power load [6].

The 3D thermal analysis is used to study the transformers. In [7] the local losses are initially estimated from electromagnetic field analysis based on the Finite Element Method (FEM), then it use a method for recalculating the loss distribution based on the principle that the initial rate of rise of temperature at any point is proportional to the loss generated at that point. More accurate temperature distributions within the transformer are then computed from the resulting loss density distribution. Overheating due to nonlinear loads is analyzed with 3D finite elements method too. The nonlinear FEM calculation is then combined with a mixed analytical and numerical form of the electrical circuit equation to take into account the skin and proximity effects in the rectangular windings. Then a steady state thermal FEM using the previous resultant current densities allows to characterize the temperature distribution of the transformer with nonsinusoidal currents [8]. In making the thermal simulation model, it is difficult to model a detailed structure of the toroidal inductor, part due to the calculation cost, and for this there are studies to find a compact thermal modeling method of a toroidal inductor, especially as a part for switch mode power supply [9]. The thermal models for transformers were studied using also genetic algorithms which, working on the load and on the measured hot-spot temperature pattern, permits to identify a corrected set of parameters for the thermal model of the transformer. Genetic algorithms are used for study conventional laminated transformers [10] and for toroidal core too [11]. The toroidal transformers are used in power electronic devices and their optimal design is considered to optimize the geometry, the operating frequency, the shape and the core material structure [12]. Optimizations of the toroidal inductors are studied in order to maximize frequency of a given geometry and impedance. This is important for semiconductor devices at high frequency, which also need a thermal optimization [13]. Because many equipments use the Pulse Width Modulation (PWM) inverter, there are also necessary analysis of the power loss in toroidal cores under PWM excitation [14]. An important difference between sinusoidal and PWM voltage excitation is a significant difference in the variation of instantaneous energy loss through the magnetising cycle which is also contributes to the additional losses [14]. The toroidal transformers are used from usual and small power applications to special application at high-currents, as in [15], where it is used a multi-turn primary,

A. T. Pleşca is with the Gheorghe Asachi Technical University of Iasi, Iasi, IS 700050 Romania (phone: 40-232-278683; fax: 40-232-237627; e-mail: aplesca@ee.tuiasi.ro).

single turn secondary, current step-up toroidal transformer, with 5÷10 MAmps of peak current with pulse rise-time. Therefore is essential to estimate the thermal aspects even for such a toroidal transformer type. The steady-state thermal analysis for toroidal transformers can be conducted using a lumped parameter model which can be applied to small power and distribution-grade toroidal transformers, including the effects of the number of turns of windings, number of layers, insulation properties and geometric properties of the transformer. The model can be used with different external media and encapsulation, such as air, oil and epoxy [16]. A thermal lumped parameter model for a toroidal transformer is also proposed in [17]. Based on the model, the temperature profile for the studied case is extracted and the place and the temperature of the hottest spot are obtained. It is shown, for the low loads, that the hottest spot is on the interior part of the core and, for the higher loads, the hottest spot place has been changed to the primary winding. The toroidal design of the magnetic system of the inductor allows to decrease the magnetic scattering field and to avoid butt connections of the portions of the magnetic conductor and to increase the efficiency and the power coefficient [18]. The effect of temperature on toroidal transformers is studied under no load condition into a climatic chamber to see the temperature influence on the value of RMS idle current and on the magnetization of the toroidal transformer [19]. Special applications are the toroidal HTS (high temperature superconductor) transformers. They are analyzed from the thermal point of view by means of FEM analysis [20]. The analysis was a 2D/3D harmonic electromagnetic and thermal analysis and the temperature distribution is also calculated. Based on electrical and magnetic properties, such as saturation magnetization, initial permeability, and coercivity, in [21] are presented some considerations about the possibilities of applications of nanocrystalline alloys in toroidal cores for current transformers. From the magnetic characterization and the computational simulations, using FEM, it has been verified that the nanocrystalline alloys properties reinforce the hypothesis that the use of these materials in cores can reduce the ratio and phase errors and can also improve its accuracy class. Even the acoustic noise is studied for the toroidal transformers in audio and video equipment under normal and adverse mains conditions [22].

This study attempts to achieve and validate a three dimensional thermal model for a power toroidal transformer in different operating conditions.

## II. THERMAL MODEL

The aim of this study is to develop a three dimensional thermal model of a power toroidal transformer. The basic equation of heat transfer has the following expression for each volume element  $dV$ :

$$Q_c = Q_t - Q_r \quad (1)$$

The left term of the equation is the heating power from the current flow,  $Q_c$ . It is in balance with the heat stored by temporal change of temperature  $Q_t$ , the power removed from the element by thermal conduction  $Q_r$ . For the above thermal power quantities, the following equations can be written:

$$\begin{aligned} Q_c &= \iiint \rho j^2 dV; & Q_t &= \iiint \gamma c \frac{\partial \theta}{\partial t} dV; \\ Q_r &= \iiint \text{div}(\lambda \cdot \text{grad} \theta) dV \end{aligned} \quad (2)$$

where:

- $\rho$  means the electrical resistivity;
- $j$  – current density;
- $\gamma$  – material density;
- $c$  – specific heat;
- $\lambda$  – thermal conductivity;
- $\theta$  – temperature;
- $\theta_a$  – ambient temperature.

Therefore,

$$\iiint \rho j^2 dV = \iiint \gamma c \frac{\partial \theta}{\partial t} dV - \iiint \text{div}(\lambda \cdot \text{grad} \theta) dV \quad (3)$$

The material density, specific heat and thermal conductivity do not have an important temperature variation; thus they can be regarded as constants. On the other hand, the electrical resistivity has a significant temperature variation and can be estimated through a parabolic variation or a linear one. In general, the difference between these two types of variation is not so important. For the electrical resistivity we may consider a linear variation with the temperature,

$$\rho = \rho_0 [1 + \alpha(\theta - \theta_a)] \quad (4)$$

where  $\alpha$  is the coefficient of electrical resistivity variation with temperature. Considering the notation:

$$g = \theta - \theta_a \quad (5)$$

The following relation is obtained:

$$\iiint \rho_0 (1 + \alpha g) j^2 dV = \iiint \gamma c \frac{\partial g}{\partial t} dV - \iiint \text{div}(\lambda \cdot \text{grad} g) dV \quad (6)$$

The above equation into cylindrical coordinates becomes:

$$\begin{aligned} \iiint \rho_0 (1 + \alpha g) j^2 dV &= \iiint \gamma c \frac{\partial g}{\partial t} dV - \\ &- \iiint \lambda \left( \frac{1}{r} \frac{\partial g}{\partial r} + \frac{\partial^2 g}{\partial r^2} + \frac{1}{r^2} \frac{\partial^2 g}{\partial \varphi^2} + \frac{\partial^2 g}{\partial z^2} \right) dV \end{aligned} \quad (7)$$

with the coordinates transform from cartesian to cylindrical ones,

$$x = r \cos\varphi; \quad y = r \sin\varphi; \quad z = z \quad (8)$$

In steady state conditions, the heat storage term is zero, and the equation (7) becomes,

$$\iiint \rho_0 (1 + \alpha \vartheta) j^2 dV = - \iiint \lambda \left( \frac{1}{r} \frac{\partial \vartheta}{\partial r} + \frac{\partial^2 \vartheta}{\partial r^2} + \frac{1}{r^2} \frac{\partial^2 \vartheta}{\partial \varphi^2} + \frac{\partial^2 \vartheta}{\partial z^2} \right) dV \quad (9)$$

Because the physical parameters, especially the electrical resistivity, vary with the temperature, the above equation is a non-linear type with variable coefficients and it demands a numerical procedure to evaluate the temperature distribution. It is desirable to restate the problem by considering various forms of discretization. The discretised form of the problem only requires the solution to be satisfied at a finite number of points in the region; and in the remainder of the region, appropriate interpolations may be used. Thus, this case is reduced to an algebraic form involving only the basic arithmetic operations, which could in turn be solved by numerical methods. These methods have become very accurate and reliable for solving initial and boundary value problems. The basic idea of the finite element method is to discretise the main domain into several subdomains, or finite elements. These elements can be irregular and possess different properties so that they form a basis to discretise complex structures, or structures with mixed material properties.

A three dimensional model for a toroidal transformer has been developed using specific software like Pro-ENGINEER, which is an parametric, integrated 3D CAD/CAM/CAE solution. The parametric modeling approach uses parameters, dimensions, features, and relationships to capture intended product behavior and create a recipe which enables design automation and the optimization of design and product development processes. Pro Engineer provides a complete set of design, analysis and manufacturing capabilities on one, integral, scalable platform. These required capabilities include solid modelling, surfacing, rendering, data interoperability, routed systems design, simulation, tolerance analysis and tooling design.

Toroidal electromagnetic devices (coils, toroidal transformers, magnetic amplifiers, frequency multiplier, controlled inductive reactance, etc.), have the following features:

- the magnetic field in the core has the highest value on the circumference of radius  $r_m$  and the smallest one on radius  $R_m$  so that saturation gradually evolves from inside out;
- thermal load in the magnetic core unit volume is variable and appropriate in all the volume;
- winding thickness is variable, unfavorable to cooling so that unitary thermal load from the volume is variable with values increased at the interior where heat transfer is more difficult;

- inner winding is made turn near turn, Fig. 1, with overlapping layers, while at the outside can be combined turns of different layers from the inside, filling coefficients inner  $k_{ui}$  and outer  $k_{ue}$ , being different;
- the toroidal wind up position (vertical, horizontal, somewhat), affects the cooling of the winding and the maximum heating zone.

The subject was a power toroidal transformer with rated voltage about 230V and rated power of 1kVA. The magnetic circuit has a square cross-section of 50mm x 50mm, the inner diameter of 100mm and the outer diameter of 200mm. The three-dimensional thermal model has been achieved with the following simplifying assumptions:

- primary and secondary winding were modeled by geometric toroidal bodies with appropriate sizes which consist of magnetic core, without rounding the interior and exterior edges;
- both windings, primary and secondary, have been modelled as toroidal component parts with high thickness towards inside part of the transformer because of technological reasons;
- insulation on the magnetic core, between the windings and the outer one, were modelled also through toroidal geometric bodies with thickness provided by the manufacturer, but without rounding the interior and exterior edges.

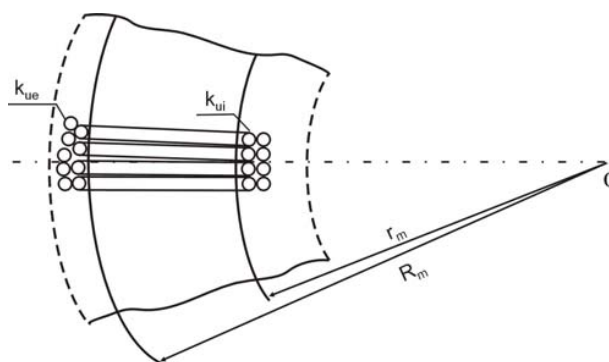


Fig. 1 Constructive features of the toroidal winding

The 3D model had taken into consideration the following component parts of a toroidal transformer: magnetic core, inside insulation, primary winding, the insulation between primary and secondary winding, secondary winding, outside insulation, as shown in Fig. 2.

Also, to measure temperatures in accordance with the thermocouples' positioning, there were marked the points TMAXIMUM, maximum temperature, on the magnetic core at mid-height, in the inner part, TAVERAGE, the average temperature between the primary and secondary winding at half height, and TSURFACE temperature on the toroidal surface, also at half of the height, inside of the transformer, according to Fig. 2.

### III. THERMAL SIMULATIONS

The Pro-MECHANICA software has been used for all thermal simulations. Pro-MECHANICA uses adaptive p-element technology whereas conventional finite element codes use non-adaptive h-element technology. The underlying geometry can be followed more precisely. The elements use a polynomial equation to describe the stress shape function, which can vary from 3<sup>rd</sup> to 9<sup>th</sup> order.

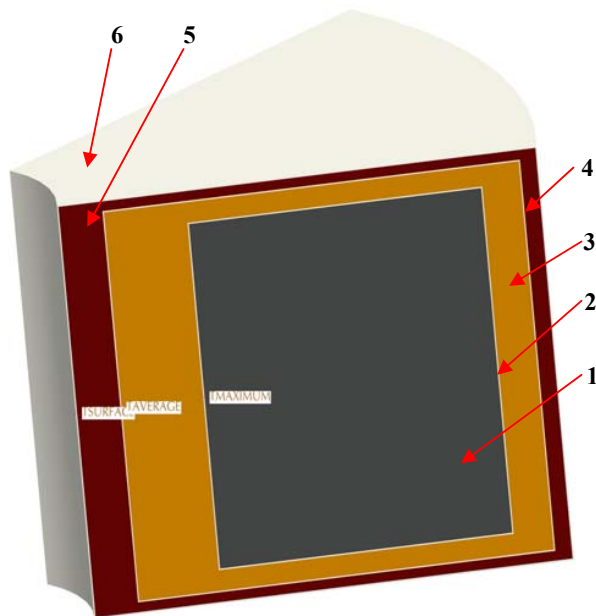


Fig. 2 Thermal model of toroidal transformer (1 - magnetic core, 2 - magnetic core insulation, 3 - primary winding, 4 - insulation between windings, 5 - secondary winding, 6 - external insulation)

This means that fewer elements are required and they can follow high stress gradients very closely. It also means that a tetrahedral solid mesh in Pro-MECHANICA is likely to give more reliable results than a tetrahedral solid mesh in other codes, where often a brick mesh would be required. The automatic convergence strategy can be employed, whereby the polynomial order of the elements is increased rather than having to re-mesh with smaller elements. Actually, an automated solution strategy is used whereby an initial run, or pass as it is termed in Pro-MECHANICA, is conducted with the p-orders set to a low value for speed of response, and then the p-orders are automatically raised to a higher level in areas of high stress gradient or where greater accuracy is required. This achieves the ideal combination of accuracy and efficiency, whilst being virtually operator-independent with regard to meshing technique. Furthermore Pro-MECHANICA has built-in optimisation capabilities, so that designs can be optimised efficiently and automatically.

It was considered a real application when this type of power transformer is used to supply a proper resistive load. To perform thermal simulations there were specified the materials with appropriate parameters to the geometrical volumes in the

thermal model, data summarized in the Table I, in accordance with the guidelines specified in Fig. 2. From experimental tests, it was obtained the coefficient of overall heat transmission,  $k_t = 9.35 \text{ W/}^\circ\text{Cm}^2$ , necessary to apply the boundary condition, at an ambient temperature of  $20^\circ\text{C}$ . Knowing the values of the primary winding resistances,  $0.37\Omega$ , and the secondary one,  $17\text{m}\Omega$ , it has been calculated the thermal loads for some values of the primary currents (6 and 9A) and secondary ones (34 and respectively, 50A) achieving the following values for primary thermal loads: 13.32; 29.97W and 19.65; 42.5W for secondary thermal loads. It was considered an uniform distribution of thermal load throughout the whole volume occupied by the primary and secondary winding.

TABLE I  
MATERIAL DATA AND COEFFICIENTS AT  $20^\circ\text{C}$  IN CORRELATION WITH COMPONENT PARTS FROM FIG. 2

Parameter	Material		
	Copper (3, 5)	Magnetic material (1)	Polyimide insulation (2, 4, 6)
$\gamma \text{ (kg/m}^3\text{)}$	8900	8400	1420
$c \text{ (J/kg}^\circ\text{C)}$	385	370	1090
$\lambda \text{ (W/m}^\circ\text{C)}$	385	10	0.12

The mesh of this 3D toroidal transformer thermal model has been done using tetrahedron solids element types with the following allowable angle limits (degrees): maximum edge: 170; minimum edge: 5; maximum face: 174.3; minimum face: 5. The maximum aspect ratio was 23.45 and the maximum edge turn (degrees): 95. The single pass adaptive convergence method to solve the thermal steady-state simulation has been used.

Further on, some steady state thermal simulations have been done. The temperature distribution on the toroidal transformer is presented in Fig. 3. In Fig. 4 and Fig. 5 is shown the temperature distribution through 50% vertical cross-section and 50% horizontal cross-section, respectively, of the same power toroidal transformer. It is to observe the highest temperatures to inner side of the transformer because of the higher copper mass and thermal volume density respect to the outer side of the transformer.

Radial and axial temperature distribution of the toroidal transformer at different electric currents flowing through primary and secondary windings, are presented from Fig. 6 to Fig. 9. Temperature distribution along the radius and axis of the toroidal transformer for different ambient temperature, at 50A secondary current, is shown in Fig. 10 and Fig. 11.

### IV. DISCUSSION OF THE RESULTS

In Fig. 6, the temperature distribution along the radius of the toroidal transformer at a secondary current of 50 A (primary current of 9A), is shown. It can be observed the maximum temperature ( $\theta_{\text{sim\_max}}$ ) about  $75^\circ\text{C}$  at half distance of the transformers' height. The maximum temperature corresponds to the inner area between primary winding and the magnetic core. This is explained because of

the higher thickness of the primary and secondary windings towards the inner area of the transformer. Also, the thermal load is higher at inner part of the toroidal transformer. To extremities, it can be noticed a higher value of the temperature on the inside surface ( $\theta_{sim\_max} = 62\text{ }^{\circ}\text{C}$ ) respect to the outside surface temperature ( $\theta_{sim\_max} = 53.4\text{ }^{\circ}\text{C}$ ). This is

explained because of the more favourable cooling conditions at outside surface of the transformer.

There is also the radial temperature distribution for the upper surface ( $\theta_{sim\_sup} = 60.8\text{ }^{\circ}\text{C}$ ) and bottom surface ( $\theta_{sim\_inf} = 60.41\text{ }^{\circ}\text{C}$ ). It can be observed close values both for maximum temperature and extremities temperatures.

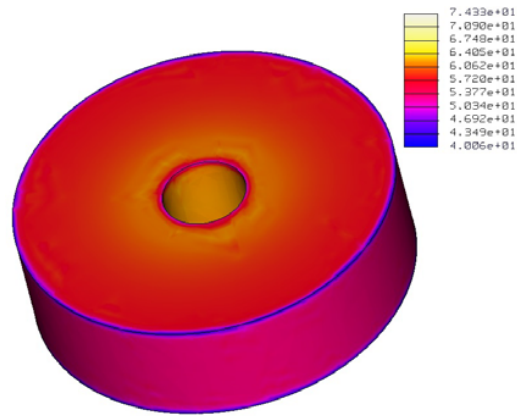


Fig. 3 Temperature distribution on the toroidal transformer

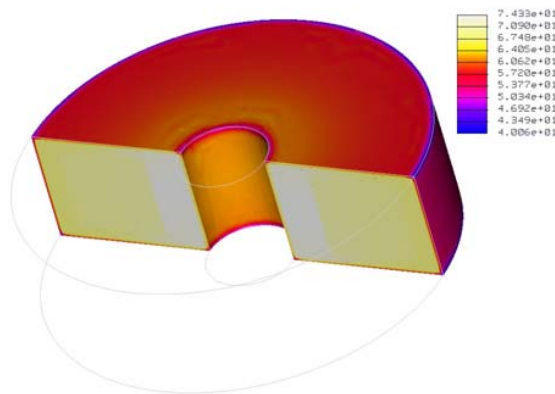


Fig. 4 Temperature distribution of the toroidal transformer (50% vertical cross-section)

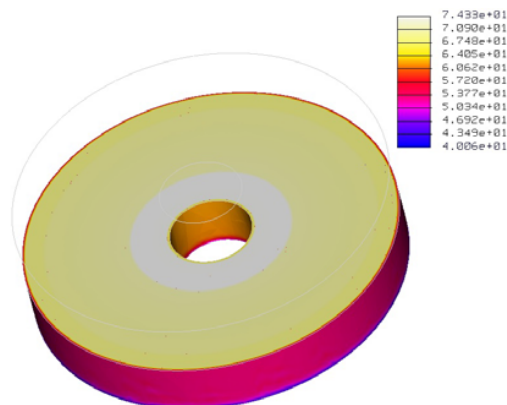


Fig. 5 Temperature distribution of the toroidal transformer (50% horizontal cross-section)

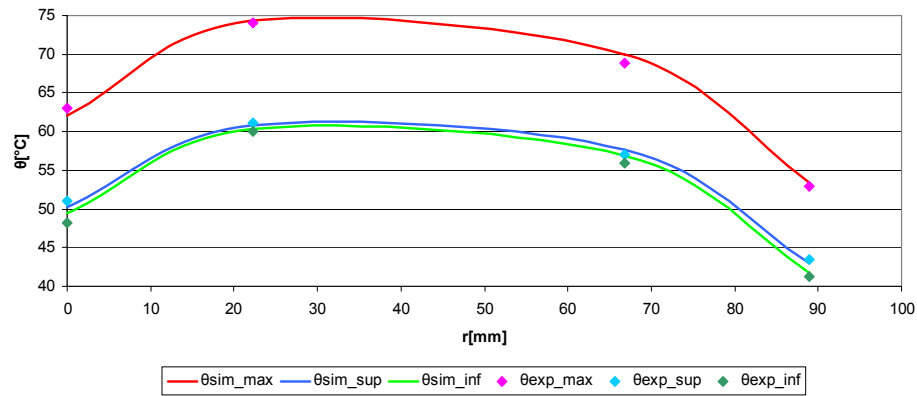


Fig. 6 Radial temperature distribution through the toroidal transformer at secondary current of 50 A. Comparison between simulation values ( $\theta_{sim\_max}$ ,  $\theta_{sim\_sup}$ ,  $\theta_{sim\_inf}$ ) and experimental results ( $\theta_{exp\_max}$ ,  $\theta_{exp\_sup}$ ,  $\theta_{exp\_inf}$ )

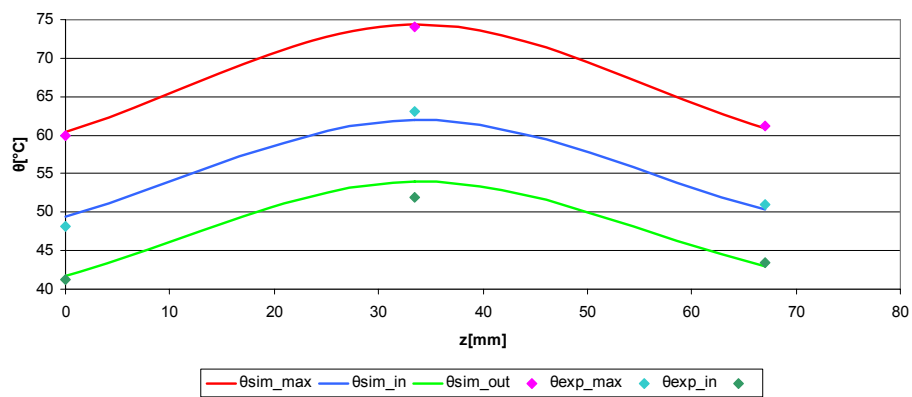


Fig. 7 Axial temperature distribution of the toroidal transformer at secondary current of 50 A. Comparison between simulation values ( $\theta_{sim\_max}$ ,  $\theta_{sim\_in}$ ,  $\theta_{sim\_out}$ ) and experimental results ( $\theta_{exp\_max}$ ,  $\theta_{exp\_in}$ ,  $\theta_{exp\_out}$ )

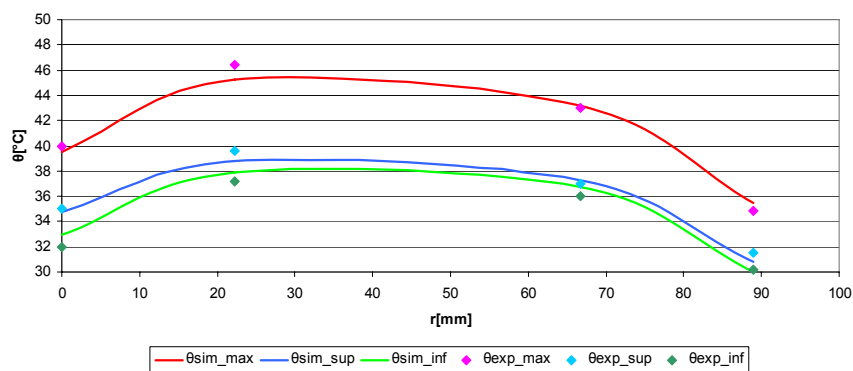


Fig. 8 Radial temperature distribution through the toroidal transformer at secondary current of 34 A. Comparison between simulation values ( $\theta_{sim\_max}$ ,  $\theta_{sim\_sup}$ ,  $\theta_{sim\_inf}$ ) and experimental results ( $\theta_{exp\_max}$ ,  $\theta_{exp\_sup}$ ,  $\theta_{exp\_inf}$ )

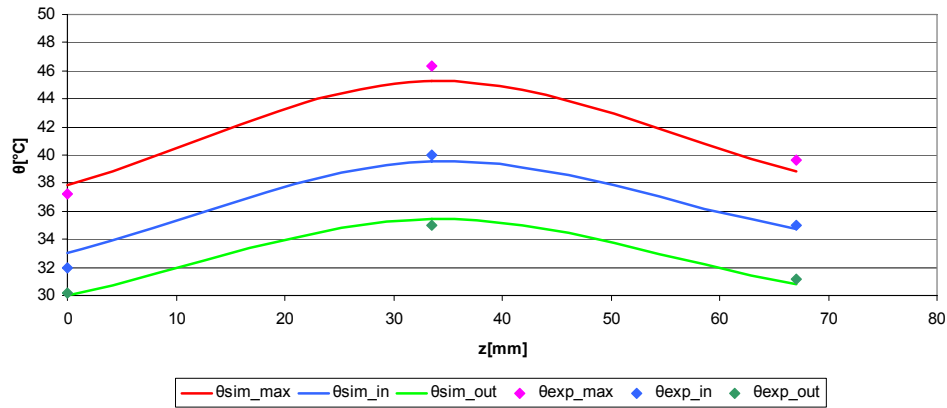


Fig. 9 Axial temperature distribution of the toroidal transformer at secondary current of 34 A. Comparison between simulation values ( $\theta_{sim\_max}$ ,  $\theta_{sim\_in}$ ,  $\theta_{sim\_out}$ ) and experimental results ( $\theta_{exp\_max}$ ,  $\theta_{exp\_in}$ ,  $\theta_{exp\_out}$ )

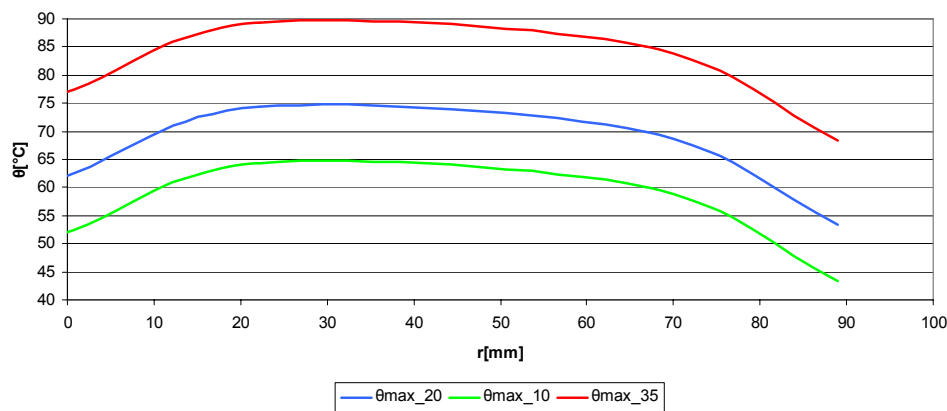


Fig. 10 Radial temperature distribution through the toroidal transformer at secondary current of 50 A for different ambient temperatures (10, 20 and 35 °C)

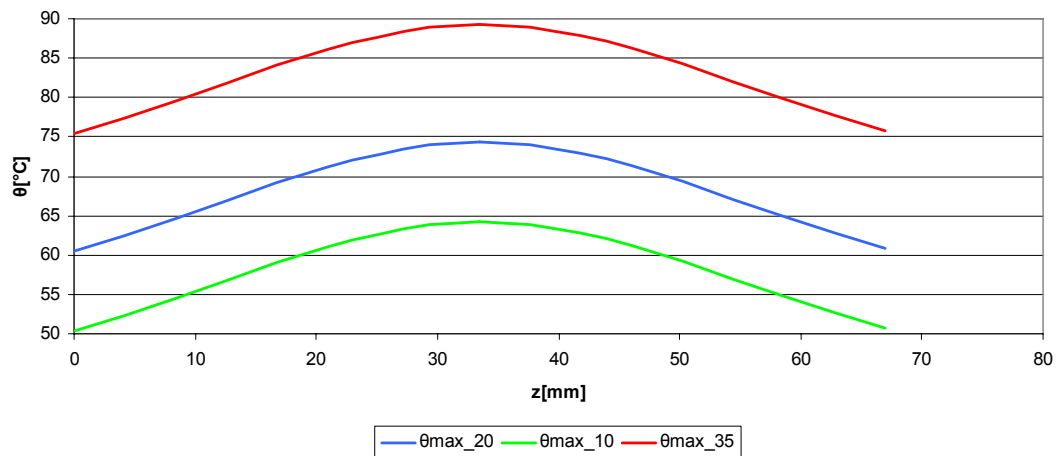


Fig. 11 Axial temperature distribution of the toroidal transformer at secondary current of 50 A for different ambient temperatures (10, 20 and 35 °C)

There are higher temperature values in the case of upper surface respect to the bottom surface because of the natural ascending warm air. The axial temperature distribution at the same secondary current of 50 A, is shown in Fig. 7.

The reference  $z = 0$ , means the bottom surface of the toroidal transformer. It can be noticed the maximum temperature ( $\theta_{sim\_max} = 75\text{ }^{\circ}\text{C}$ ) at the half distance of the transformers' height and close values of the extremities temperatures,  $\theta_{sim\_max} = 60.8\text{ }^{\circ}\text{C}$  on the upper surface and  $\theta_{sim\_max} = 60.41\text{ }^{\circ}\text{C}$  on the bottom surface of the transformer. Important temperature values are lengthwise of the inside surface of the transformer, from the low value of  $\theta_{sim\_in} = 49.4\text{ }^{\circ}\text{C}$ , maximum of  $\theta_{sim\_in} = 62\text{ }^{\circ}\text{C}$  to the high value of  $\theta_{sim\_in} = 50.3\text{ }^{\circ}\text{C}$  on the upper surface of the transformer. As expected, the lower temperature values are lengthwise axis of the outside surface of the transformer, where there is a maximum of  $\theta_{sim\_out} = 54\text{ }^{\circ}\text{C}$  at the half distance of the transformers' height. The temperature difference between inside and outside surfaces of the toroidal transformer is because higher thermal load distribution at inner transformer and more favourable cooling conditions on the outside surface of the transformer.

In Fig. 8, the temperature variation along the radius of the toroidal transformer at the secondary current of 34A (primary current of 6A), is presented. Similar to the previous case, it can be observed the maximum temperature ( $\theta_{sim\_max} = 45.28\text{ }^{\circ}\text{C}$ ) in the inner area close to the magnetic core. The temperature on the inside surface ( $\theta_{sim\_max} = 39.55\text{ }^{\circ}\text{C}$ ) is higher than on the outside surface ( $\theta_{sim\_max} = 35.47\text{ }^{\circ}\text{C}$ ). There are close temperature values on the upper surface ( $\theta_{sim\_sup} = 38.82\text{ }^{\circ}\text{C}$ ) and bottom surface ( $\theta_{sim\_inf} = 37.87\text{ }^{\circ}\text{C}$ ). The temperature curves' shape is similar as in the case with secondary current of 50A.

The axial temperature distribution at the same secondary current of 34 A, is presented in Fig. 9. As in the case with secondary current of 50 A, the maximum temperature is recorded at half of the transformers' height inside the inner area between primary winding and magnetic core ( $\theta_{sim\_max} =$

$45.28\text{ }^{\circ}\text{C}$ ). On the inside transformer surface there is maximum  $\theta_{sim\_in} = 39.55\text{ }^{\circ}\text{C}$  higher than the maximum value on the outside surface  $\theta_{sim\_out} = 35.46\text{ }^{\circ}\text{C}$ . All the obtained temperature values have been considered for an ambient temperature of  $20\text{ }^{\circ}\text{C}$ .

The temperature variations along the radius and axis of the toroidal transformer for different ambient temperatures (10, 20 and  $35\text{ }^{\circ}\text{C}$ ), are depicted in Fig. 10 and Fig. 11. The electric current has been maintained at a constant value, 50A in the secondary side. It is to observe that the temperature variation curve is translated on vertical direction depending on the temperature ambient values.

To validate the 3D thermal model some experimental tests have been done in the same conditions as in the case of thermal simulation. The electric circuit diagram used for experimental tests is shown in Fig. 12. The switch K, allow to supply with low-voltage the auto-transformer ATR, which adjusts the input voltage for the toroidal transformer TT. On the secondary side of the toroidal transformer TT, there is connected the resistive load R. The electric currents through the primary and secondary windings are measured by the ammeters  $A_1$  and  $A_2$ , respectively.

Using proper thermocouples Th, type K, it has measured the temperature on the surface of the external insulation. The measurement points are the same as during the thermal simulations. The small voltage signals provided by thermocouples have been amplified using a signal conditioning board type AT2F-16. The amplified signal was the input for a data acquisition board type PC-LPM-16 connected to a PC with the following characteristics: analogue inputs: 16 (8 differential channels), 12 bits resolution, sampling rate  $250\text{ kS/s}$ ; analogue outputs: 2, on 12 bits; digital inputs/outputs: 8; counters / timers: 2, on 24 bits; triggering: analogue, digital, start/stop; advanced control, PID adjustment, specific functions incorporated.

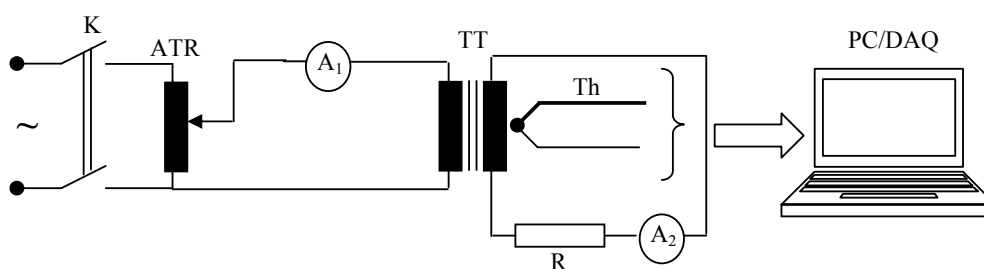


Fig. 12 Main electric diagram for experimental tests



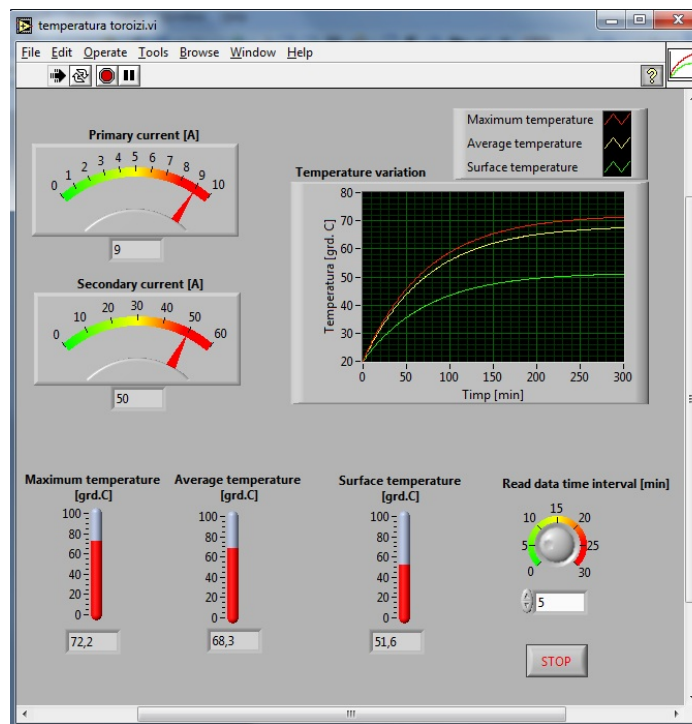


Fig. 13 LabVIEW front panel of the virtual instrument for experimental tests

The data acquisition board can be programmed using the specialized graphical software environment, LabVIEW. The front panel with the LabVIEW application used at temperature and current measurements is presented in Fig. 13.

As can be seen from the figure, the front panel allows measurement of the current from the primary and secondary of the toroidal transformer and the maximum temperatures between windings and on the transformer' surface, which are the analogue inputs to be subject to a value of maximum 10Vdc, for protection in voltage of the data acquisition board. It can also be set the reading interval of the temperature values, depending on the time constant of toroidal transformers. It can be recorded the time evolution of the temperatures; instantaneous values (maximum, average, on the surface of the transformer) are displayed on the front panel of the application, Fig. 13. The comparisons between simulation and experimental results are presented from Fig. 6 to Fig. 9. It can be noticed a good correlation between simulation results and experimental values. The differences between the temperature values resulting from experimental tests and those obtained during simulations are due to various factors: measurement errors, thermal model simplifications and mounting test conditions. The thermal model has not included the different types of busbar/conductor connections which can lead to significant heat dissipation rate. Nevertheless, the maximum difference between the experimental and simulation results is less than 3°C.

## V.CONCLUSION

The obtained three dimensional thermal model allow analysis of the thermal behaviour of power toroidal transformers. The thermal model provides the transformer temperature distribution at different currents and ambient temperature values and could be used as a designing tool for the power transformers, especially in the case of power distribution system. Some experimental tests have been made in order to validate the proposed three dimensional thermal model. There is a good correlation between experimental and simulated results. Using the proposed thermal model, the toroidal transformer design process can be improved and there is the possibility of obtaining new solutions for an optimal power management of different types of power transformers or autotransformers.

## ACKNOWLEDGMENT

This work was supported by CNC SIS – UEFISCDI, project number 610 PNII – CAPACITATI, 2013.

## REFERENCES

- [1] Hernandez, F. de Leon, and P. Gomez, "Design formulas for the leakage inductance of toroidal distribution transformers," IEEE Trans. on Power Delivery, vol. 26, pp. 2197-2204, 2011.
- [2] M.T. Askari, M. Z. A. Ab. Kadir, and M. Izadi, "On the trend of improvement of thermal model for calculating the TOT and HST," Przegląd Elektrotechniczny, vol. 88, pp. 297-301, 2012.
- [3] V. Madzarević, I. Kapetanović, M. Tešanović, and M. Kasumović, "Different approach to thermal modeling of transformers - a comparison

- of methods," *Int. J. of Energy and Environment*, vol. 5, pp. 610-617, 2011.
- [4] M.C. Popescu, N.E. Mastorakis, and L. Popescu-Perescu, "New aspects providing transformer models," *Int. J. of Systems Applications, Engineering & Development*, vol. 2, pp. 53-63, 2009.
  - [5] E.I. Amoiralis, M.A. Tsili, and A.G. Kladas, "Transformer design and optimization: a literature survey," *IEEE Trans. On Power Delivery*, vol. 24, pp. 1999-2024, 2009.
  - [6] A. Folvarcny, and M. Marek, "Experimental analysis of temperature influence on the parameters of the current load type toroidal transformers, compared with conventional types of transformers," in *11th Int. Sci. Conf. on Electric Power Engineering*, Brno, 2010, pp. 727-731.
  - [7] C.C. Hwang, P.H. Tang, and Y.H. Jiang, "Thermal analysis of high-frequency transformers using finite elements coupled with temperature rise method," *IEE Proc. - Electric Power Applications*, vol. 152, pp. 832-836, 2005.
  - [8] A. Lefevre, L. Miegerville, J. Fouladgar, and G. Olivier, "3-D computation of transformers overheating under nonlinear loads," *IEEE Trans. on Magnetics*, vol. 41, pp. 1564-1567, 2005.
  - [9] K. Koizumi, and M. Ishizuka, "Thermal modeling of toroidal inductor," *J. Nihon Kikai Gakkai Nenji Taikai Koen Ronbunshu*, vol. 6, pp. 299-300, 2005.
  - [10] V. Galdi, L. Ippolito, A. Piccolo, and A. Vaccaro, "Parameter identification of power transformers thermal model via genetic algorithms," *Electric Power Systems Research*, vol. 60, pp. 107-113, 2001.
  - [11] N. Tutkun, "Genetic estimation of iron losses in strip wound toroidal cores under PWM flux conditions," *J. of Magnetism and Magnetic Materials*, vol. 300, pp. 506-518, 2006.
  - [12] O. Nimet, G. Grellet, H. Morel, J.J. Rousseau, and D. Ligot, "Optimal design of a toroidal transformer fed by nonsinusoidal high frequency currents," in *8th Int. Conf. on Power Electronics and Variable Speed Drives*, 2000, pp. 57-62.
  - [13] C.R. Sullivan, W. Li, P. Prabhakaran, and S. Lu, "Design and fabrication of low-loss toroidal air-core inductors," in *IEEE Power Electronics Specialists Conf.*, 2007, pp. 1754-1759.
  - [14] A.J. Moses, and N. Tutkun, "Investigation of power loss in wound toroidal cores under PWM excitation," *IEEE Trans. on Magnetics*, vol. 33, pp. 3763-3765, 1997.
  - [15] P.J. Turchi, W.A. Reass, C.L. Rousculp, D.M. Oro, F.E. Merrill, J.R. Griego, et al., "Evaluation of conductor stresses in a pulsed high-current toroidal transformer," in *17th IEEE Int. Pulsed Power Conf.*, Washington DC, 2009, pp. 372-377.
  - [16] S. Purushothaman, and F. de Leon, "Heat-transfer model for toroidal transformers," *IEEE Trans. on Power Delivery*, vol. 27, pp. 813-820, 2012.
  - [17] M.A. Saket, B. Jandaghi, M. Moghaddami, and H. Oraee, "Thermal lumped parameter modeling of a toroidal transformer," in *Electric Power Engineering & Control Systems 2011*, Lviv, 2011, pp. 1-6.
  - [18] A.V. Serikov, and T.V. Gerasimenko, "Thermal calculation of transformer-type radiator," *Russian Electrical Engineering*, vol. 82, pp. 371-376, 2011.
  - [19] A. Folvarčny, M. Marek, and R. Holčáková, "Magnetic properties of types of core for toroidal transformers made from thin low-loss sheets and thermal influence on resulting transformer idle current," *J. of Electrical Engineering*, vol. 61, pp. 137-140, 2010.
  - [20] B. Grzesik, M. Stepień and R. Jez, "Toroidal HTS transformer with cold magnetic core – analysis with FEM software," *J. of Physics: Conf. Series: 9th European Conf. on Applied Superconductivity*, 2009, pp. 1-8.
  - [21] B.A. Luciano, J.M. Cavalcante de Albuquerque, W. Benício de Castro, and C.R.M. Afonso, "Nanocrystalline material in toroidal cores for current transformer: analytical study and computational simulations," *Materials Research*, vol. 8:4, pp. 395-400, 2005.
  - [22] M. Van der Veen, F. de Leon, B. Gladstone, and V. Tatu, "Measuring acoustic noise emitted by power transformers," in *AES 109th Convention*, Los Angeles, 2000, pp. 1-19.



**Adrian Pleșca** was born in Iasi, Romania, on April 16, 1972. He graduated from the Gheorghe Asachi Technical University of Iași and he received the PhD degree in Electrical Engineering in 2001. His

employment experience included the Gheorghe Asachi Technical University of Iasi, Power Engineering Department. His special fields of interest included electrical apparatus, special equipment for power semiconductor devices protection and 3D modelling and simulation of the electrical apparatus. Dr. Pleșca received Golden and Silver Medals at World Exhibition of Invention, Research and Industrial Innovation, Brussels, Belgium, EUREKA, 2001, 2004, Special Prize awarded by National Research Council of Thailand for Fundamental Research at The First International Invention's Day Convention, Bangkok, Thailand 2008, Gold Medal at 4th International Warsaw Invention Show 2010, Diploma and Genius Medal at 2nd International Invention Exhibition, Ljubljana, 2010 and Gold Prize at Seoul International Invention Fair, Korea 2011.